Searching for an intermediate-mass black hole in the blue compact dwarf galaxy MRK 996

Monthly Notices of the ROYAL ASTRONOMICAL SOCIETY

Mon. Not. R. Astron. Soc. **413,** 1729–1734 (2011) doi:10.1111/j.1365-2966.2011.18248.x

Searching for an intermediate-mass black hole in the blue compact dwarf galaxy MRK 996

A. Georgakakis,[1★] Y. G. Tsamis,[2,3] B. L. James[4] and A. Aloisi[4]

[1]*National Observatory of Athens, V. Paulou & I. Metaxa 11532, Greece*
[2]*European Southern Observatory, Karl-Schwarzschild-Str. 2, 85748 Garching, Germany*
[3]*Department of Physics and Astronomy, The Open University, Walton Hall, Milton Keynes MK7 6AA*
[4]*Space Telescope Science Institute, 3700 San Martin Drive, Baltimore, MD 21218, USA*

Accepted 2010 December 21. Received 2010 December 21; in original form 2010 September 14

ABSTRACT

The possibility is explored that accretion on an intermediate-mass black hole contributes to the ionization of the interstellar medium of the compact blue dwarf galaxy MRK 996. *Chandra* observations set tight upper limits (99.7 per cent confidence level) in both the X-ray luminosity of the posited active galactic nucleus (AGN), $L_X(2\text{–}10\,\mathrm{keV}) < 3 \times 10^{40}\,\mathrm{erg\,s^{-1}}$, and the black hole mass, $\lesssim 10^4\,\lambda^{-1}\,\mathrm{M_\odot}$, where λ is the Eddington ratio. The X-ray luminosity upper limit is insufficient to explain the high-ionization line [O IV] 25.89 μm, which is observed in the mid-infrared spectrum of MRK 996 and is proposed as evidence for AGN activity. This indicates that shocks associated with supernova explosions and winds of young stars must be responsible for this line. It is also found that the properties of the diffuse X-ray emission of MRK 996 are consistent with this scenario, thereby providing direct evidence for shocks that heat the galaxy's interstellar medium and contribute to its ionization.

Key words: galaxies: active – galaxies: dwarf – galaxies: individual: MRK 996 – X-rays: galaxies.

1 INTRODUCTION

Understanding how supermassive black holes (SBHs) grow and how they relate to the formation of their host galaxies are challenges for modern astrophysics. BHs with masses $\approx 10^9\,\mathrm{M_\odot}$ have now been observed out to $z \approx 6$, when the Universe was only about 1 Gyr old (e.g. Fan et al. 2006). Simulations can produce such monsters at early epochs by postulating violent high-accretion-rate events triggered by mergers of gas rich galaxies (e.g. Volonteri & Rees 2005). These simulations, however, have to assume seed BHs, which form very early in the Universe ($z \approx 20$) and which will eventually grow to masses as high as $10^9\,\mathrm{M_\odot}$ via accretion. The mass distribution of the seed BHs is an important parameter of the simulations. The remnants of the first stars that formed in the Universe (Population III) are believed to produce BHs with masses up to $10^3\,\mathrm{M_\odot}$ (Abel, Bryan & Norman 2000; Bromm, Coppi & Larson 2002). In this case, however, accretion well in excess of the Eddington rate is required to grow those seeds to $\approx 10^9\,\mathrm{M_\odot}$ in less than 1 Gyr (e.g. Volonteri & Rees 2005; Begelman, Volonteri & Rees 2006). An alternative scenario for the formation of seed BHs is the direct collapse of pre-galactic gas discs (Lodato & Natarajan 2006, 2007). This model produces BHs with masses up to $10^6\,\mathrm{M_\odot}$, orders of magnitude more massive than Population III stars, thereby significantly relaxing the requirements for super-Eddington accretion. A powerful probe of the seed BH population at early epochs is intermediate-mass BHs ($\lesssim 10^6\,\mathrm{M_\odot}$) in the local Universe, which are expected to reside in low-mass galaxies (i.e. M_{BH}–σ relation; Ferrarese & Merritt 2000; Gebhardt et al. 2000; Greene et al. 2010; Graham et al. 2011). Volonteri, Lodato & Natarajan (2008), for example, argue that the BH occupation number of dwarf galaxies can constrain models of the origin of the seed BHs in the early Universe, for example, Population III stars versus direct collapse of pre-galactic gas discs.

The dynamical signatures of moderate-size BHs are hard to detect with current instrumentation. As a result, searches for such objects in nearby galaxies have turned to the easier but less-direct approach of finding active galactic nuclei (AGNs) in small or bulgeless galaxies, that is, BHs during their active stage. NGC 4395 and POX 52 are the best-studied examples of nearby broad-line AGNs with an estimated BH mass of about $10^5\,\mathrm{M_\odot}$ (Filippenko & Ho 2003; Barth et al. 2004; Peterson et al. 2005). Furthermore, optical spectroscopic studies have recently found evidence for type-2 AGN activity associated with intermediate-mass BHs in the late-type spirals NGC 1042 (Seth et al. 2008; Shields et al. 2008), UGC 6192 (Barth, Greene & Ho 2008) and NGC 3621 (Barth et al. 2009). Systematic efforts to compile samples of moderate-size BHs have also been carried out by Greene & Ho (2004, 2007) and Dong et al.

★E-mail: age@astro.noa.gr

(2007). Those studies used the SDSS spectroscopic data base to identify galaxies with AGN signatures in their optical spectra and estimated BH masses of $<10^6\,M_\odot$. The hosts of those AGNs are typically late-type galaxies with stellar masses $<10^{10}\,M_\odot$.

A special class of low-mass galaxies which have attracted much attention over the years is blue compact dwarfs (BCDs). These systems are exceptional because of their low metallicities (1/40–1/3 solar) and high specific star formation rates, which indicate one of the first major episodes of star formation. BCDs are therefore unique laboratories for testing theories of galaxy formation. They resemble the first galaxies that formed in the early Universe out of gas with near-primordial metallicity, and which according to the standard hierarchical formation paradigm are the building blocks of massive galaxies. An important recent development in the study of BCDs has been the suggestion that they harbour AGNs associated with intermediate-mass BHs. If true, then this would offer the opportunity to study in detail the parallel formation of the first stars and the seed BHs in systems that resemble protogalaxies.

Evidence for AGN activity in BCDs includes the incidence of dense ionized cores ($>10^4$ cm^{-3}), broad Balmer emission lines with widths in excess of 2000 km s^{-1} (Izotov, Thuan & Guseva 2007; Izotov & Thuan 2008) and high-ionization narrow optical emission lines suggesting the presence of a hard ionizing continuum (Thuan & Izotov 2005; James et al. 2009). The evidence for AGNs in BCDs, however, is far from conclusive. Broad and high-excitation lines can be due to stellar activity, for example, shocks in fast winds of young massive stars (e.g. Izotov, Thuan & Guseva 2007; Thuan, Hunt & Izotov 2008; James et al. 2009). Unfortunately, optical emission-line diagnostic diagrams (e.g. Baldwin, Phillips & Terlevich 1981; Kewley et al. 2001), which have traditionally been used to separate stellar photoionization – dominated from AGNs – excited sources, break down at the low-metallicity regime (Groves, Heckman & Kauffmann 2006), and hence cannot be applied to BCDs. The most-reliable method for confirming or refuting the presence of an AGN in any galaxy, irrespective of metallicity, is X-ray observations. The detection of an X-ray point source at the nuclear regions of a galaxy is strong evidence for accretion on to a massive compact object.

In this paper, we explore the X-ray properties of MRK 996, a BCD that is among the prime candidates for hosting an AGN. Mid-infrared (mid-IR) spectroscopy of MRK 996 with the *Spitzer*/IRS shows the [O IV] 25.89 μm line with an ionization potential of 54.9 eV, indicating the presence of a hard continuum (Thuan et al. 2008), which could be produced by an AGN. Optical integral field spectroscopy by the VLT/VIMOS has revealed an extremely dense nuclear region (electron density $\approx 10^7$ cm^{-3}), much denser than in typical BCDs (James et al. 2009). Also, a very red point source ($J - K = 1.8$) was found at the position of the nucleus of the galaxy, while photometry with *Spitzer* indicates hot dust in the central galaxy regions and a mid-IR spectral energy distribution similar to that of Seyferts (Thuan et al. 2008). New *Chandra* observations of MRK 996 are presented in this paper and are used to search for AGN signatures in this galaxy. We adopt a distance of 22.3 Mpc for MRK 996, which corresponds to a velocity of 1642 km s^{-1} (James et al. 2009) and $H_0 = 73.5$ km s^{-1} Mpc^{-1}.

2 DATA PROCESSING

MRK 996 was observed for a total of 50 ks with the Advanced CCD Imaging Spectrometer (ACIS-S) camera aboard *Chandra* on 2009 August 3. The ACIS-S was operated in very faint mode and the target was placed at the nominal aimpoint of the S3 CCD. The data were reduced using the CIAO (Chandra Interactive Analysis of Observations) package version 4.1.2 and the methodology described in Laird et al. (2009). The first step was to produce the level 2 event file from the raw data. Hot pixels and cosmic-ray afterglows were flagged. The charge-transfer inefficiency and time-dependent gain corrections were then applied and the ACIS pixel randomization was removed. As MRK 996 was observed in very faint mode, the ACIS particle background cleaning algorithm was also applied. The data were inspected for high particle background periods and it was found that they were not affected. Images were constructed in four energy bands 0.5–7.0 keV (full), 0.5–2.0 keV (soft), 2.0–7.0 keV (hard) and 4.0–7.0 keV (ultrahard). Sources were detected using the methodology described in Laird et al. (2009). The final source list consists of sources with Poisson probabilities $<4 \times 10^{-6}$ in at least one of the energy bands defined above. Source-free background maps and sensitivity maps were also constructed as described in Georgakakis et al. (2008).

The astrometry of the *Chandra* data was refined by comparing the positions of X-ray sources with those of optical galaxies in the *HST* Wide Field Planetary Camera 2 (WFPC2) observations presented by Thuan et al. (1996). The astrometric accuracy of the *HST* image is 0.25 arcsec. Excluding sources within the optical radius of MRK 996 (0.3 arcmin) obtained from the Third Reference Catalogue of Bright Galaxies (RC3; de Vaucouleurs et al. 1991), there are only two X-ray sources within the *HST*/WFPC2 field of view. Both of them are associated with optical galaxies. Comparison of the optical and X-ray source positions shows small systematic offsets of δ RA = 0.25 arcsec and δ Dec. = 0.05 arcsec, which were applied to the X-ray source catalogue and images.

3 X-RAY POINT SOURCES

At the Poisson probability threshold of 4×10^{-6}, two X-ray point sources are detected within the optical radius of MRK 996 (0.3 arcmin). Fig. 1 (left-hand panel) overplots the positions of the two sources on the *HST* image of MRK 996. Neither is associated with the nucleus of the galaxy. Relative to the optical centre of MRK 996, one of the point sources lies ≈7 arcsec to the south and the other ≈6 arcsec to the north. The southern X-ray detection is likely associated with one of the globular clusters of MRK 996. It lies ≈0.15 arcsec from an optical point source on the *HST* image of the galaxy identified as a globular cluster by Thuan et al. (1996).

The X-ray fluxes and luminosities of the two point sources are estimated from their X-ray spectra. The specextract task of the CIAO package was employed to extract the counts at the positions of each source, to estimate background spectra and to generate the redistribution matrix function and the ancillary response file. Source spectra were grouped to have at least 1 count per bin. The spectral analysis was carried out within the XSPEC v12 package. As the net counts are low for both sources (see Table 1), we fit the data with a simple power-law model absorbed by cold gas in our Galaxy. A Galactic hydrogen column density of $N_{\rm H} = 4 \times 10^{20}$ cm^{-2} was adopted using the H I map of Kalberla et al. (2005). In XSPEC terminology, our model is wabs × po, where wabs is the cold absorption from our Galaxy and po is the power law. The derived parameters are listed in Table 1. We assess the probability that the two off-nuclear X-ray sources are background AGNs. We use the 0.5–10 keV $\log N - \log S$ relation of Georgakakis et al. (2008) to estimate the expected number of sources brighter than 10^{-15} erg s^{-1} cm^{-2} within a radius of ≈7 arcsec from the optical centre of MRK 996. The flux limit above corresponds to the approximate 0.5–10 keV flux of the faintest of the two sources. The radius cut is the maximum angular distance of the two point sources from the galaxy centre. The expected

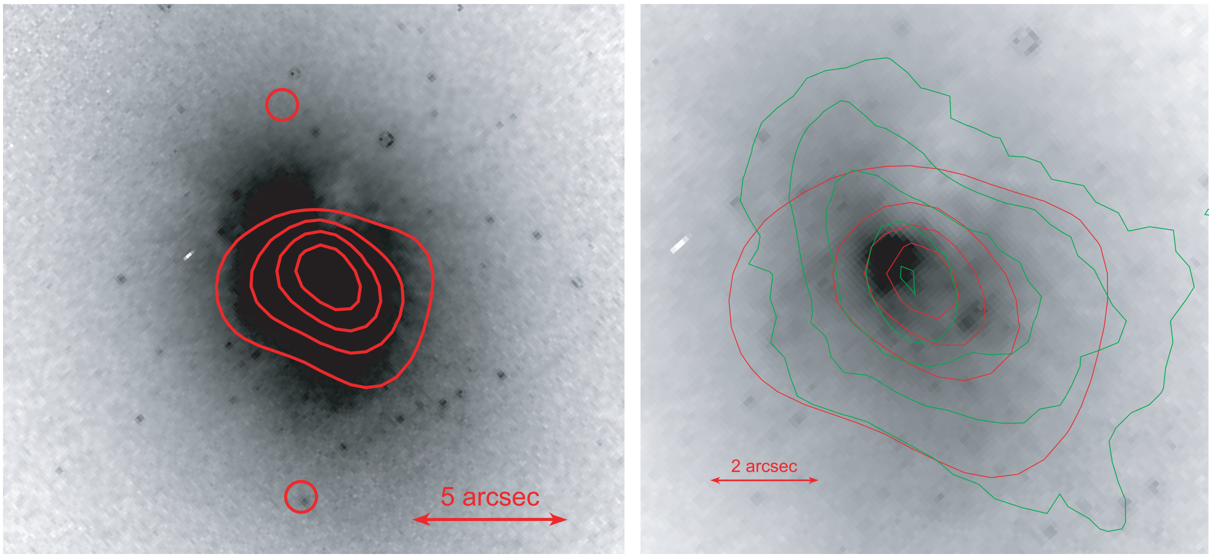

Figure 1. Left-hand panel: *HST F569W* filter image of MRK 996. The circles are 0.5 arcsec in radius and mark the positions of the X-ray point sources detected in the *Chandra* observations. The contours correspond to the diffuse X-ray emission of MRK 996. North is up and east is left. Right-hand panel: close-up of the nuclear regions of MRK 996 to compare the spatial distributions of the hot X-ray-emitting gas versus the optically detected H II gas. The grey-scale is the *HST F569W* filter image, the red contours correspond to the diffuse X-ray component (same contours as in the left-hand image) and the green contours are the narrow components of the Hα emission line from the integral field spectroscopic observations described by James et al. (2009).

Table 1. MRK 996 point-source spectral parameters. Columns are (1) CXO ID; (2) total counts within the extraction region; (3) best-fitting photon index of the power-law model; (4) the c-statistic value of the fit and degrees of freedom (d.o.f.); (5) flux in the 0.3–10 keV band; and (6) X-ray luminosity in the 0.3–10 keV band.

ID	Total counts	Γ	c-statistics/d.o.f.	f_X(0.3–10 keV) (10^{-14} erg s^{-1} cm^{-2})	L_X(0.3–10 keV) (erg s^{-1})
CXO J012735.6−061930	74	4.0 ± 0.6	33.7/24	$2.0^{+1.0}_{-0.6}$	$1.2^{+0.6}_{-0.4} \times 10^{39}$
CXO J012735.5−061943	11	$2.5^{+2.1}_{-1.6}$	8.9/9	$0.3^{+0.2}_{-0.1}$	$1.8^{+1.2}_{-0.6} \times 10^{38}$

number of background sources is 0.12. The Poisson probability of two background AGNs within ≈7 arcsec of the MRK 996 nuclear regions is 1.8×10^{-4}. We conclude that both X-ray point sources are likely to be associated with MRK 996.

4 DIFFUSE EMISSION

The nuclear regions of MRK 996 are dominated by diffuse X-ray emission. We explore the morphology of the X-ray gas by first removing point sources and then adaptively smoothing the full-band X-ray image using the cmooth task of CIAO. The X-ray contours of the smoothed image are overplotted on the *HST* observations in Fig. 1. The peak of the diffuse X-ray emission lies in between the nuclear star-forming region and an optical point source in the south-west which was proposed to be a young star cluster by Thuan et al. (1996). There is also tentative evidence, limited by small photon statistics, that the distribution of the diffuse component is more extended in the southern direction. This is interesting, if it is confirmed by deeper X-ray observations, as the spatial distribution of globular clusters of MRK 996 also appears to be asymmetric in the same direction. Most of them are found in the south of the galaxy (Thuan et al. 1996). Fig. 1 (right-hand panel) also shows that the spatial distribution of the diffuse X-ray component and the H II ionized gas is similar.

The X-ray spectrum of the diffuse component has been extracted using the specextract task of CIAO which is the proposed tool in the case of extended sources. The extraction aperture has a radius of about 2 arcsec and encompasses most of the diffuse component photons. The background spectrum was determined from nearby source-free regions. The spectrum was fitted with a hot thermal plasma model (Raymond & Smith 1977) which is absorbed by cold gas in our Galaxy with an H I column density of $N_{\rm H} = 4 \times 10^{20}$ cm^{-2}. The X-ray spectrum and the best-fitting model are shown in Fig. 2. Table 2 lists the hot gas parameters estimated from the best-fitting model to the data. The temperature of the thermal plasma, about 1 keV (≈10^7 K), is higher than the typical temperatures of the diffuse hot gas in dwarf starbursts (e.g. Ott, Walter & Brinks 2005) and other BCDs (Thuan et al. 2004).

5 DISCUSSION

5.1 Is there an AGN in MRK 996?

One of the motivations for the *Chandra* observations of MRK 996 was to explore the possibility that an AGN is responsible for the excitation of the mid-IR [O IV] 25.89 μm line reported by Thuan et al. (2008). Below about 2 keV the nuclear regions of the galaxy are dominated by diffuse hot gas, which renders the search for a point source in the soft and full bands difficult. The hard band (2–7 keV) is less contaminated by the diffuse X-ray emission. We therefore estimate a conservative upper limit [99.7 per cent confidence level (CL)] for the flux of a point source at the optical centre of MRK 996,

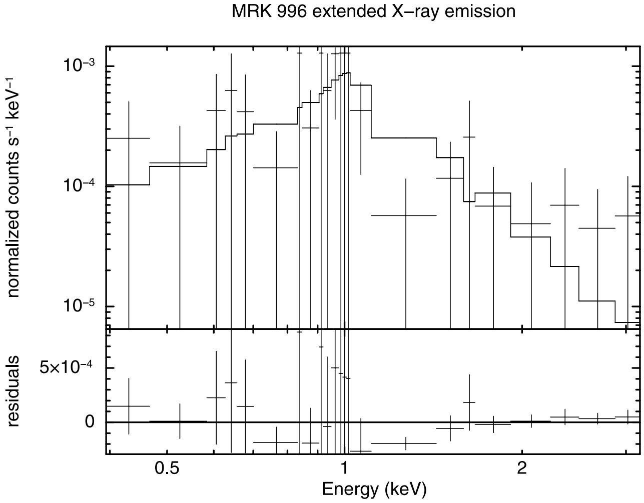

Figure 2. Spectrum of the diffuse X-ray emission of MRK 996. The best-fitting thermal plasma model is shown with the histogram. The residuals of the model are also plotted. There are 25 counts within the extracted region. The c-statistic of the fit is 13.9 for 21 degrees of freedom.

assuming that the observed counts at that position are from a nuclear X-ray point source.

For the estimation of the upper limits, we adopt a Bayesian methodology similar to that described in Laird et al. (2009). For a source with an observed number of total counts N (source and background) within the 70 per cent encircled energy fraction radius and a local background value B, the probability of flux f_X is

$$P(f_X, N) = \frac{T^N e^{-T}}{N!}, \quad (1)$$

where $N = S + B$ and $S = f_X \times t_{exp} \times C \times \eta$. In the latter equation, t_{exp} is the exposure time at a particular position after accounting for instrumental effects (i.e. exposure map), C is the conversion factor from the flux to count rate which depends on the adopted model for the spectrum of the source and η is the encircled energy fraction, that is, 0.7 in our case. The integral of $P(f_X, N)$ gives the probability that the flux of the source is lower than $f_{X,U}$, that is, the CL for the flux upper limit:

$$\int_{f_{X,L}}^{f_{X,U}} P(f_X, N)\,df_X = \mathrm{CL}. \quad (2)$$

The lower limit of the integration is $f_{X,L} = 10^{-18}\,\mathrm{erg\,s^{-1}\,cm^{-2}}$. Equation (2) is then solved numerically to estimate the flux upper limit that corresponds to the confidence interval of 99.7 per cent. For the flux-to-count rate conversion factor, we adopt two extreme values. The first corresponds to a power law with $\Gamma = 1.9$ and represents the case of an unabsorbed AGN. The second is for a reflection-dominated spectrum, which is approximated by the pexrav model of XSPEC (Magdziarz & Zdziarski 1995) and represents the case of a Compton thick AGN ($N_H \gtrsim 10^{24}\,\mathrm{cm^{-2}}$). The 99.7 per cent upper limit is $f_X(2\text{–}10\,\mathrm{keV}) = 6 \times 10^{-15}\,\mathrm{erg\,s^{-1}\,cm^{-2}}$ for the $\Gamma = 1.9$ model and $10^{-14}\,\mathrm{erg\,s^{-1}\,cm^{-2}}$ for the reflection-dominated spectrum. The 2–10 keV luminosity 99.7 per cent upper limits are, respectively, 3.5×10^{38} and $6 \times 10^{38}\,\mathrm{erg\,s^{-1}}$. In the case of a reflection-dominated spectrum, we assume that the intrinsic luminosity of the source is 50 times higher ($3 \times 10^{40}\,\mathrm{erg\,s^{-1}}$), as the reflected emission is believed to represent 2 per cent of the direct component (e.g. Gilli, Comastri & Hasinger 2007). The corresponding upper limits for the BH mass are $\lesssim 100\lambda^{-1}\,\mathrm{M_\odot}$ in the case of no obscuration and $\lesssim 10^4\,\lambda^{-1}\,\mathrm{M_\odot}$ for Compton thick obscuring clouds, where λ is the Eddington ratio. In this calculation, a bolometric-to-hard X-ray luminosity ratio of 35 is adopted (Elvis et al. 1994).

The luminosity upper limits above should be compared with the AGN luminosity required to explain the [O IV] 25.89 μm line in the mid-IR spectrum of MRK 996 reported by Thuan et al. (2008). Those authors modelled this line with an AGN ionization spectrum of the form $f_\nu \propto \nu^{-1}$ and estimated a total rate of ionizing photons $\log Q(H) = 51.125$. Assuming the photons are distributed in the energy interval 1–1000 Ry, this rate translates to a 2–10 keV intrinsic AGN luminosity of $4.5 \times 10^{40}\,\mathrm{erg\,s^{-1}}$. This is 2 dex higher than the 99.7 luminosity upper limit in the case of an unabsorbed AGN. This indicates that an unabsorbed or mildly absorbed active SBH cannot be responsible for the ionization of the [O IV] 25.89 μm line. If the central engine in MRK 996 is absorbed by Compton thick material and the X-ray emission is dominated by the reflected component, the estimated 99.7 per cent upper limit for the intrinsic luminosity of the AGN is still lower compared to that required to explain the [O IV] 25.89 μm line. We conclude that the X-ray data provide

Table 2. The gas parameters for the thermal plasma model used to fit the spectrum of the diffuse emission of MRK 996. The parameters are estimated for a metallicity $Z_{opt} = 0.5\,\mathrm{Z_\odot}$ determined by James et al. (2009) from the optical emission-line spectrum of MRK 996 and a volume-filling factor $f_v = 1$. The parameter values can be converted to lower filling factors and other metallicities using the scaling relation given in this table, where $\xi = Z/Z_{opt}$. The listed parameters are: (1) best plasma temperature in keV; (2) the normalization of the best-fitting model, which equals $10^{-14}(4\pi D^2)^{-1} \int n_e n_H\,dV$, where D is the distance to MRK 996 in cm, n_e and n_H are, respectively, the electron and proton densities in $\mathrm{cm^{-3}}$; (3) the plasma temperature in K; (4) the 0.3–10 keV X-ray luminosity in $\mathrm{erg\,s^{-1}}$; (5) the mean electron density in $\mathrm{cm^{-3}}$ estimated from the normalization of the best-fitting model, assuming that the proton and electron densities are equal; (6) pressure of the hot gas estimated from the relation $P/k = 2\,n_e\,T$; (7) the gas thermal energy, $E_{th} = 3n_e\,VkT$, where V is the volume of the X-ray-emitting region, which is assumed to be a sphere of 2 arcsec = 214 pc radius at the source distance (i.e. similar to the extraction region of the X-ray spectrum of the diffuse component); (8) the total mass of the hot gas estimated from the relation $M_{hot} = n_e\,m_p\,V$, where m_p is the proton mass; (9) gas cooling time, $t_{cool} = E_{th}/L_X$; and (10) X-ray emissivity estimated from the relation $\Lambda_X = L_X/(\mathrm{norm} \times 4\,\pi D^2 \times 10^{14})$.

Parameter	Value
kT (keV)	$1.1 \pm ^{+0.4}_{-0.2}$
norm (10^{-6})	$1.8^{+0.9}_{-0.7}$
T (10^7 K)	$1.3 \pm ^{+0.5}_{-0.2}$
L_X(0.3–10 keV) ($10^{38}\,\mathrm{erg\,s^{-1}}$)	$1.1 \pm ^{+0.6}_{-0.4}$
$\langle n_e \rangle$ [$\times\,(f\,\xi)^{-0.5}$] ($\mathrm{cm^{-3}}$)	$0.10^{+0.03}_{-0.02}$
P/k [$\times\,(f_v\,\xi)^{-0.5}$] ($10^6\,\mathrm{K\,cm^{-3}}$)	$2.7^{+1.4}_{-0.7}$
E_{th} [$\times\,f_v^{0.5}\,\xi^{-0.5}$] ($10^{53}$ erg)	$5.2^{+3.6}_{-1.9}$
M_{hot} [$\times\,f_v^{0.5}\,\xi^{-0.5}$] ($10^5\,\mathrm{M_\odot}$)	$0.8^{+0.3}_{-0.2}$
t_{cool} [$\times\,f_v^{0.5}\,\xi^{-0.5}$] ($10^8$ yr)	$1.5^{+1.1}_{-0.4}$
Λ ($10^{-23}\,\mathrm{erg\,s^{-1}\,cm^3}$)	$1.0^{+0.7}_{-0.5}$

evidence against AGN ionization for the [O IV] 25.89 μm line at a significance level of about 99.7 per cent.

Hao et al. (2009) propose a new diagnostic diagram for studying the dominant excitation mechanism of galaxies which is based on the mid-IR emission-line ratios [O IV]25.89 μm/[S III]33.48 μm and [Ne III]15.56 μm/[Ne II]12.81 μm. They showed that AGN and pure starbursts bifurcate on this diagram with AGNs having higher [O IV]25.89 μm/[S III]33.48 μm line ratios. Using the fluxes for the relevant emission lines from Thuan et al. (2008), we estimate for MRK 996 [O IV]25.89 μm /[S III]33.48μm = 0.11 ± 0.06 and [Ne III]15.56 μm/[Ne II]12.81 μm = 2.8 ± 0.3. These ratios place MRK 996 in the starburst branch of the Hao et al. (2009) diagnostic diagram, further suggesting that the ionization of the [O IV]25.89 μm line is not because of an AGN.

5.2 Origin of the diffuse component

An alternative explanation for the [O IV] 25.89 μm line is ionization via shocks (Thuan et al. 2008) associated with stellar outflows and supernova explosions. Shock excitation has already been proposed to partly explain the broad component of the optical emission lines in MRK 996 (James et al. 2009). The shocks generated by starburst winds are also known to carve bubbles of hot (10^6–10^7 K) and overpressured gas in the interstellar medium (ISM), which can be observed at soft X-rays (e.g. Ott et al. 2005).

We explore the possibility of a superbubble for the observed diffuse X-ray emission by comparing the observed X-ray luminosity of the hot gas, as determined from the X-ray spectral analysis of Section 4, with the predictions of the bubble models of Castor, McCray & Weaver (1975), Weaver et al. (1977) and Mac Low & McCray (1988):

$$L_X = \int_0^{R_{max}} n(r)^2 \, \Lambda_X(T, Z) \, dV, \qquad (3)$$

where $\Lambda_X(T, Z)$ is the X-ray volume emissivity of the gas and $n(r)$ is the radial density profile of the bubble. Substituting in the integral above the $n(r)$ relation of Chu et al. (1995) and $\Lambda_X(T, Z)$ estimated from the observations (see Table 2), we find

$$L_X = 2.6 \times 10^{34} \, I \, L_{37}^{33/35} \, n_0^{17/35} \, t_6^{19/35} \quad (\mathrm{erg\,s^{-1}}), \qquad (4)$$

where L_{37} is the mechanical luminosity of the starburst in units of 10^{37} erg s^{-1}, n_0 is the number density of the ambient ISM in cm^{-3} and t_6 is the age of the starburst in Myr. The dimensionless integral I has a value of about 2 (see Chu et al. 1995). We do not include an explicit dependence on metallicity in equation (4) as in Chu et al. (1995). Such a dependence is accounted for in the calculation of $\Lambda_X(T, Z)$ through the normalization of the thermal plasma model fit to the spectrum of the diffuse X-ray component.

For the estimation of the mechanical luminosity injected by the winds of young stars and supernova explosions, we use the STARBURST99 stellar evolution synthesis model (Leitherer et al. 1999; Vázquez & Leitherer 2005). We adopt a continuous star formation model for the starburst with a Salpeter initial mass function (lower mass 1 M$_\odot$, upper mass 100 M$_\odot$, slope 2.35) and star formation rate of 1 M$_\odot$ yr^{-1} and metallicity $Z = 0.008$, that is, similar to the 0.5 Z$_\odot$ metallicity of MRK 996 (James et al. 2009). The model mechanical luminosity is then scaled to the star formation rate of MRK 996, for which we adopt the value 1.3 M$_\odot$ yr^{-1}. This was estimated from the integral field spectroscopy observations presented by James et al. (2009) by integrating the narrow-line component of the Hα emission line under the assumption that the broad component of this line is associated with shocks. James et al. (2009) estimated an age for the young stellar population in MRK 996 of 3–5 Myr based on the equivalent width of the Hβ line. An average starburst age of 4 Myr is adopted in equation (4). Under those assumptions, the mechanical luminosity from the STARBURST99 model is 3.9×10^{40} erg s^{-1} cm^{-2} (fig. 112 of Leitherer et al. 1999). For the density of the ambient ISM, James et al. (2009) estimate $n_0 =$ 1–40 cm^{-3} for the outer regions of MRK 996 based on the [S II] λ6716/λ6731 intensity ratio. In ionized nebulae, however, the [S II] emission is typically associated with lower ionization gas which would be expected to be of higher density than the average. It is therefore likely that the lower end of the n_0 range determined by James et al. (2009) represents the mean ISM density into which the superbubble expands. Adopting $n_0 = 1$ cm^{-3} we predict an X-ray luminosity of 3×10^{38} erg s^{-1}, larger than the observed one, 1.1×10^{38} erg s^{-1}. However, given the large uncertainties in the model parameters (e.g. a slightly younger age of 3 Myr yields $L_X = 7 \times 10^{37}$ erg s^{-1}) and the observables [e.g. $\Lambda_X(T, Z)$, metallicity of the X-ray-emitting gas, ISM density], we conclude that the observed L_X of the diffuse component is broadly consistent with the expanding bubble model prediction.

We caution that the diffuse component could be the result of the combined emission of high-mass X-ray binaries (HMXRBs) that lie below the sensitivity limit of the *Chandra* observations. We assess the contribution of such sources by integrating the global luminosity function of HMXRBs in starburst galaxies determined by Grimm, Gilfanov & Sunyaev (2003). A star formation rate of 1.3 M$_\odot$ yr^{-1} is adopted for MRK 996 (James et al. 2009) and the integration is carried out between 10^{37}–10^{38} erg s^{-1}. The upper limit is the approximate 0.5–10 keV band point-source sensitivity limit of the *Chandra* observations. We estimate a total X-ray luminosity for HMXRBs below the *Chandra* data detection threshold of $\approx 10^{39}$ erg s^{-1}. In principle, the diffuse X-ray component could be attributed to HMXRBs. The X-ray spectrum of the diffuse component is not inconsistent with this interpretation. The best-fitting spectral index of the power-law component is 2.2 ± 0.7. Although HMXRBs typically have flatter X-ray spectra, ≈1.2 (e.g. White, Swank & Holt 1983), systems with spectral indices as steep as $\Gamma \approx 2$ have been observed (e.g. Sasaki, Pietsch & Haberl 2003). Although it is hard to reject the possibility of X-ray binaries dominating the diffuse component, there are arguments against this interpretation. The age of the starburst in MRK 996 is 3–5 Myr (James et al. 2009), while models of the evolution of the X-ray luminosity of HMXRBs (e.g. Sipior 2003; Linden et al. 2010) predict that these sources peak at later times, ≈10–20 Myr after the initial burst, especially in the case of low-metallicity systems. It is also interesting that the peak of the diffuse X-ray emission falls between the nuclear starburst and the young superstar cluster candidate in the south-west of the nucleus identified by Thuan et al. (1996). One could reasonably assume that the peak emission is associated with an interaction region where the respective stellar wind superbubbles from the two sources collide and heat the ISM.

6 CONCLUSIONS

Chandra X-ray observations are used to search for an AGN in the BCD MRK 996, which could explain the high-ionization line [O IV] 25.89 μm observed in the mid-IR spectrum of the galaxy. The estimated upper limit for the X-ray luminosity of a nuclear point source in MRK 996 is inconsistent with AGN ionization being responsible for the excitation of the [O IV] 25.89 μm line. Shock excitation must be responsible for this line. We find direct evidence for shocks by studying the diffuse X-ray emission of MRK 996.

The properties of this component are broadly consistent with shock heating from stellar winds and supernova explosions. A tight upper limit of $\lesssim 10^4\ \lambda^{-1}\ M_\odot$ is also set for the posited BH mass of MRK 996.

ACKNOWLEDGMENTS

AG acknowledges financial support from the Marie-Curie Reintegration Grant PERG03-GA-2008-230644. YGT acknowledges the award of a Marie Curie intra-European Fellowship within the 7th European Community Framework Programme (grant agreement PIEF-GA-2009-236486). Support for this work was provided by the National Aeronautics and Space Administration (NASA) through Chandra Award Number 11700503 issued by the Chandra X-ray Observatory Center, which is operated by the Smithsonian Astrophysical Observatory for and on behalf of the NASA under contract NAS8-03060.

REFERENCES

Abel T., Bryan G. L., Norman M. L., 2000, ApJ, 540, 39
Baldwin J. A., Phillips M. M., Terlevich R., 1981, PASP, 93, 5
Barth A. J., Ho L. C., Rutledge R. E., Sargent W. L. W., 2004, ApJ, 607, 90
Barth A. J., Greene J. E., Ho L. C., 2008, AJ, 136, 1179
Barth A. J., Strigari L. E., Bentz M. C., Greene J. E., Ho L. C., 2009, ApJ, 690, 1031
Begelman M. C., Volonteri M., Rees M. J., 2006, MNRAS, 370, 289
Bromm V., Coppi P. S., Larson R. B., 2002, ApJ, 564, 23
Castor J., McCray R., Weaver R., 1975, ApJ, 200, L107
Chu Y., Chang H., Su Y., Mac Low M., 1995, ApJ, 450, 157
de Vaucouleurs G., de Vaucouleurs A., Corwin H. G., Jr, Buta R. J., Paturel G., Fouqué P., 1991, Third Reference Catalogue of Bright Galaxies. Springer-Verlag, Berlin, Heidelberg, New York
Dong X., Wang T., Yuan W., Zhou H., Shan H., Wang H., Lu H., Zhang K., 2007, in Ho L. C., Wang J.-W., eds, ASP Conf. Ser. Vol. 373, The Central Engine of Active Galactic Nuclei. Astron. Soc. Pac., San Francisco, p. 57
Elvis M. et al., 1994, ApJS, 95, 1
Fan X. et al., 2006, AJ, 131, 1203
Ferrarese L., Merritt D., 2000, ApJ, 539, L9
Filippenko A. V., Ho L. C., 2003, ApJ, 588, L13
Gebhardt K. et al., 2000, ApJ, 539, L13
Georgakakis A., Nandra K., Laird E. S., Aird J., Trichas M., 2008, MNRAS, 388, 1205
Gilli R., Comastri A., Hasinger G., 2007, A&A, 463, 79
Graham A. W., Onken C. A., Athanassoula E., Combes F., 2011, MNRAS, doi:10.1111/j.1365-2966.2010.18045.x
Greene J. E., Ho L. C., 2004, ApJ, 610, 722
Greene J. E., Ho L. C., 2007, ApJ, 670, 92
Greene J. E. et al., 2010, ApJ, 721, 26
Grimm H., Gilfanov M., Sunyaev R., 2003, MNRAS, 339, 793
Groves B. A., Heckman T. M., Kauffmann G., 2006, MNRAS, 371, 1559
Hao L., Wu Y., Charmandaris V., Spoon H. W. W., Bernard-Salas J., Devost D., Lebouteiller V., Houck J. R., 2009, ApJ, 704, 1159
Izotov Y. I., Thuan T. X., 2008, ApJ, 687, 133
Izotov Y. I., Thuan T. X., Guseva N. G., 2007, ApJ, 671, 1297
James B. L., Tsamis Y. G., Barlow M. J., Westmoquette M. S., Walsh J. R., Cuisinier F., Exter K. M., 2009, MNRAS, 398, 2
Kalberla P. M. W., Burton W. B., Hartmann D., Arnal E. M., Bajaja E., Morras R., Pöppel W. G. L., 2005, A&A, 440, 775
Kewley L. J., Dopita M. A., Sutherland R. S., Heisler C. A., Trevena J., 2001, ApJ, 556, 121
Laird E. S. et al., 2009, ApJS, 180, 102
Leitherer C. et al., 1999, ApJS, 123, 3
Linden T., Kalogera V., Sepinsky J. F., Prestwich A., Zezas A., Gallagher J., 2010, ApJ, 725, 1984
Lodato G., Natarajan P., 2006, MNRAS, 371, 1813
Lodato G., Natarajan P., 2007, MNRAS, 377, L64
Mac Low M., McCray R., 1988, ApJ, 324, 776
Magdziarz P., Zdziarski A. A., 1995, MNRAS, 273, 837
Ott J., Walter F., Brinks E., 2005, MNRAS, 358, 1453
Peterson B. M. et al., 2005, ApJ, 632, 799
Raymond J. C., Smith B. W., 1977, ApJS, 35, 419
Sasaki M., Pietsch W., Haberl F., 2003, A&A, 403, 901
Seth A., Agüeros M., Lee D., Basu-Zych A., 2008, ApJ, 678, 116
Shields J. C., Walcher C. J., Böker T., Ho L. C., Rix H., van der Marel R. P., 2008, ApJ, 682, 104
Sipior M. S., 2003, PhD thesis, The Pennsylvania State University
Thuan T. X., Izotov Y. I., 2005, ApJS, 161, 240
Thuan T. X., Izotov Y. I., Lipovetsky V. A., 1996, ApJ, 463, 120
Thuan T. X., Bauer F. E., Papaderos P., Izotov Y. I., 2004, ApJ, 606, 213
Thuan T. X., Hunt L. K., Izotov Y. I., 2008, ApJ, 689, 897
Vázquez G. A., Leitherer C., 2005, ApJ, 621, 695
Volonteri M., Rees M. J., 2005, ApJ, 633, 624
Volonteri M., Lodato G., Natarajan P., 2008, MNRAS, 383, 1079
Weaver R., McCray R., Castor J., Shapiro P., Moore R., 1977, ApJ, 218, 377
White N. E., Swank J. H., Holt S. S., 1983, ApJ, 270, 711

This paper has been typeset from a TEX/LATEX file prepared by the author.